J|A|C|S
ARTICLES
Published on Web 11/21/2003

Characterization of Hydrogen Bonds in the Interactions between the Hydroperoxyl Radical and Organic Acids

Renato L. T. Parreira and Sérgio E. Galembeck*

Contribution from the Departamento de Química, Faculdade de Filosofia, Ciências e Letras de Ribeirão Preto, Universidade de São Paulo, Avenida dos Bandeirantes 3900, Ribeirão Preto, 14040-901 SP, Brazil

Received June 23, 2003; E-mail: segalemb@usp.br

Abstract: The hydrogen bonds formed between the hydroperoxyl radical and formic, acetic, and trifluoroacetic acids were characterized using geometric, energetic, and electronic parameters through calculations done with the UB3LYP/6-311++G (3df,3pd) and UB3LYP/EPR-III methods. The wave functions were analyzed through the natural bond orbital, natural steric analysis, natural resonance theory, and atoms in molecules methods. The energy decomposition method proposed by Xantheas was used. The vibrational frequencies and the intensity of the O−H stretching bands, as well as the spin densities, were compared with experimental evidence. The results allowed the characterization of the hydrogen bonds formed in the complexation of the acids with the hydroperoxyl radical. Complexation led to significant alterations in the equilibrium geometry of the monomers. Energetic analysis proved that the studied complexes are stable and allowed the understanding of the effect of the electron-donating and electron-withdrawing groups in their stabilization. The alterations in the electronic structure of the monomers after complexation led to an increase in the resonance of the carboxyl group, which can be partially attributed to the hydrogen bond.

Introduction

The hydrogen bond is one of the most important intermolecular interactions,[1,2] and its wide occurrence makes it an object of study in various areas such as physics, chemistry, crystallography, crystal engineering, and molecular biology, among others. It defines the properties of many materials[3] such as synthetic polymers and is responsible for (i) the tertiary structure in macromolecules, (ii) the properties of various fluids and molecular solids, and (iii) the conformational preference of a large group of molecules.[4,5] Many theoretical and practical studies involving its characterization and nature have been done.[6−8] However, a precise definition for the hydrogen bond has not yet been found.[7] On one hand, a purely electrostatic character has been attributed to these bonds, but it has been observed that such interactions can present a considerable covalent character, as shown by experimental[6] and computational[7] studies.

Emphasis has been given to the study of hydrogen bonds formed between neutral molecules and ion−molecule complexes, but the interactions between radicals and molecules has been little studied.[9] Generally, free organic radicals are very reactive,[10] but effects such as hyperconjugation and resonance can stabilize these species. Nevertheless, most of them present short lifetimes, limiting the possibility of isolating complexes where such species are present.[10] Alkorta et al.[10] have studied the ability of some carbon radicals to act as acceptors for hydrogen bonds. Geometries and energies showed that these radicals are weak acceptors for hydrogen bonds and that their strength is qualitatively related to the molecular electrostatic potential minimum of the isolated radicals.[10]

Hydrogen bonds are also important in atmospheric chemistry, especially those involving peroxyl radicals, since these species take part in reactions that lead to the formation and destruction of the ozone layer.[11] Francisco et al. have studied the interaction between the hydroperoxyl radical (**1**) and formic (**2**), acetic (**3**), and trifluoroacetic (**4**) acids.[9,12] Such interactions lead to significant alterations in geometries and vibrational frequencies. The binding energies are strong and present magnitudes similar to those of systems bound through weak covalent bonds.[12] These data indicate that these complexes belong to the partially bonded systems category, as suggested by Leopold.[13]

Since there are few papers reporting experimental or computational studies on hydrogen bonds in radicals and because hydrogen bonds between the radical **1** and the acids **2**−**4** are

* To whom correspondence should be addressed.

(1) Dkhissi, A.; Adamowicz, L.; Maes, G. *Chem. Phys. Lett.* **2000**, *324*, 127.
(2) Aquino, A. J. A.; Tunega, D.; Haberhauer, G.; Gerzabeck, M. H.; Lischka, H. *J. Phys. Chem. A* **2002**, *106*, 1862.
(3) Espinosa, E.; Molins, E. *J. Chem. Phys.* **2000**, *113*, 5686.
(4) Rappé, A. K.; Bernstein, E. R. *J. Phys. Chem. A* **2000**, *104*, 6117.
(5) Parreira, R. L. T.; Abrahão, O., Jr.; Galembeck, S. E. *Tetrahedron* **2001**, *57*, 3243.
(6) Isaacs, E. D.; Shukla, A.; Platzman, P. M.; Hamann, D. R.; Barbiellini, B.; Tulk, C. A. *Phys. Rev. Lett.* **1999**, *82*, 600.
(7) Dannenberg, J. J.; Haskamp, L.; Masunov, A. *J. Phys. Chem. A* **1999**, *103*, 7083.
(8) Ugalde, J. M.; Alkorta, I.; Elguero, J. *Angew. Chem., Int. Ed.* **2000**, *39*, 717.
(9) Francisco, J. S. *Angew. Chem., Int. Ed.* **2000**, *39*, 4570.
(10) Alkorta, I.; Rozas, I.; Elguero, J. *Ber. Bunsen-Ges. Phys. Chem.* **1998**, *102*, 429.
(11) Aplincourt, P.; Ruiz-López, M. F.; Assfeld, X.; Bohr, F. *J. Comput. Chem.* **1999**, *20*, 1039.
(12) Aloisio, S.; Francisco, J. S. *J. Am. Chem. Soc.* **2000**, *122*, 9196.
(13) Leopold, K. R.; Canagaratna, M.; Phillips, J. A. *Acc. Chem. Res.* **1997**, *30*, 57.

10.1021/ja036846v CCC: $25.00

extremely strong, the alterations in chemical bonds upon formation of such complexes have been studied in this work through the NBO (natural bond orbital), NRT (natural resonance theory), and NSA (natural steric analysis) methods proposed by Weinhold and the AIM (atoms in molecules) method. The changes in (i) the equilibrium geometries, (ii) vibrational frequencies and intensities of the O−H stretching bands, and (iii) atomic charges and spin densities of these species after complexation have been analyzed, and the energy analysis proposed by Xantheas has been employed.

Computational Methods

Optimization of geometries and vibrational frequency calculations were carried out using the GAUSSIAN 98 program,[14] employing the density functional theory with the B3LYP hybrid functional.[15−17] For the open-shell compounds, the unrestricted DFT method with the same functional (UB3LYP) was used. The basis functions 6-311++G-(3df,3pd)[18−21] and EPR-III[22] were employed. Energies were corrected with the zero-point energy (ZPE). The GAPT charges (generalized atomic polar tensor)[23] were calculated from the polar atomic tensors, which are related to the intensities of bands in the infrared spectrum.

The energetic analyses for dimers were carried out by using the method of Xantheas for many-body interactions.[24,25] The total energy (E_2) of a dimer can be decomposed as

$$E_2 \equiv \sum_{i=1}^{2} E(i) + \Delta^2 E(1,2) \tag{1}$$

In this expression, $E(i)$ are the energies of the relaxed molecules in the dimer. The two-body term is defined as

$$\Delta^2 E(1,2) = E(1,2) - \{E(1) + E(2)\} \tag{2}$$

$E(1,2)$ is the energy of the dimer. The binding energy of two bodies is

$$\mathrm{BE}_2 = E_2 - \sum_{m=1}^{2} E_m \tag{3}$$

where E_m is the energy of the monomer m in the gas phase. The relaxation energy is defined as

$$E_\mathrm{R} = \sum_{i=1}^{2} E(i) - 2E_m \tag{4}$$

and is a measure of the energy employed to distort a molecule from its equilibrium geometry to the supermolecule geometry.[24] To take into account the effects of the basis set superposition error (BSSE), the counterpoise method (CP) was employed.[26] Thus, the energy of subsystem 1 ($E(1/(1/2))$ is calculated in the geometry and in the basis functions of the complex (1,2), considering ghost orbitals for subsystem 2. The energy of the dimer can be decomposed according to eq 1, where the terms can be replaced by those corrected through BSSE.

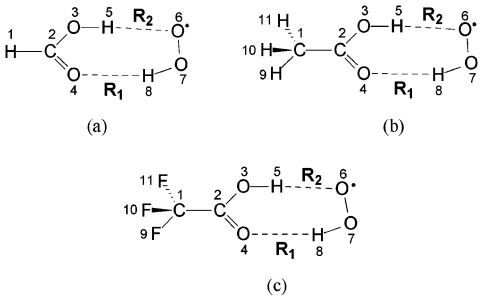

Figure 1. Numbering for isolated compounds and complexes: (a) **2**, **5**; (b) **3**, **6**; (c) **4**, **7**.

$$\Delta^2 \tilde{E}((1,2)/(1,2)) = E((1,2)/(1,2)) - \{E(1/(1,2)) + E(2/(1,2))\} \tag{5}$$

The total BSSE is the difference between the corrected and non-corrected interaction energies:

$$(\mathrm{BSSE})_n = B\tilde{E}_n - BE_n \tag{6}$$

The wave function analysis was done by using the NBO method,[27,28] including natural population analysis (NPA),[29] NSA,[30] and NRT.[31−34] These calculations were carried out using the NBO 5.0 program[35] interfaced with the GAUSSIAN 98 package. To help these analyses, the Molekel 4.1 visualization program was employed.[36]

The topological analysis of the electron density was done using the theory of AIM,[37−39] which has been employed in the characterization of hydrogen bonds in a variety of molecular complexes.[40,41] Calculations were carried out with the software suite PROAIM.[42]

Results and Discussion

The results below include the geometric, energetic, and electronic aspects involved in the hydrogen bonds that are formed when formic (**2**), acetic (**3**), and trifluoroacetic (**4**) acids are complexed with the hydroperoxyl radical (**1**). For all the studied properties, the results obtained for the basis functions 6-311++G(3df,3pd) and EPR-III were similar, and only the

(14) Frisch, M. J.; Trucks, G. W.; Schlegel, H. B.; Scuseria, G. E.; Robb, M. A.; Cheeseman, J. R.; Zakrzewski, V. G.; Montgomery, J. A.; Stratmann, R. E., Jr.; Burant, J. C.; Dapprich, S.; Millam, J. M.; Daniels, A. D.; Kudin, K. N.; Strain, M. C.; Farkas, O.; Tomasi, J.; Barone, V.; Cossi, M.; Cammi, R.; Mennucci, B.; Pomelli, C.; Adamo, C.; Clifford, S.; Ochterski, J.; Petersson, G. A.; Ayala, P. Y.; Cui, Q.; Morokuma, K.; Malick, D. K.; Radbuck, A. D.; Raghavachari, K.; Foresman, J. B.; Cioslowski, J.; Ortiz, J. V.; Stefanov, B. B.; Liu, G.; Liashenko, A.; Piskorz, P.; Komaromi, L.; Gomperts, R.; Martin, R. L.; Fox, D. J.; Keith, T. A.; Al-Laham, M. A.; Peng, C. Y.; Nanayakkara, A.; Gonzalez, C.; Challacombe, M.; Gill, P. M. W.; Johnson, B. G.; Chen, W.; Wong, M. W.; Andres, J. L.; Head-Gordon, M.; Replogle, E. S.; Pople, J. A. *Gaussian 98*; Gaussian Inc.: Pittsburgh, PA, 1998.
(15) Becke, A. D. *J. Chem. Phys.* **1993**, *98*, 5648.
(16) Lee, C.; Yang, W.; Parr, R. G. *Phys. Rev. B* **1988**, *37*, 785.
(17) Stephens, P. J.; Devlin, F. J.; Chabalowski, C. F.; Frish, M. J. *J. Phys. Chem.* **1994**, *98*, 11623.
(18) Ditchfield, R.; Hehre, W. J.; Pople, J. A. *J. Chem. Phys.* **1971**, *54*, 724.
(19) Hehre, W. J.; Ditchfield, R.; Pople, J. A. *J. Chem. Phys.* **1972**, *56*, 2257.
(20) Hariharan, P. C.; Pople, J. A. *Mol. Phys.* **1974**, *27*, 209.
(21) Frisch, M. J.; Pople, J. A.; Binkley, J. S. *Chem. Phys.* **1984**, *80*, 3265.
(22) Barone, V. In *Recent Advances in Density Functional Methods*; Chong, D. P., Ed.; World Scientific Publishing Co.: Singapore, 1995; Part I.
(23) Cioslowski, J. *J. Am. Chem. Soc.* **1989**, *111*, 8333.
(24) Xantheas, S. S. *J. Chem. Phys.* **1994**, *100*, 7523.
(25) Xantheas, S. S. *J. Chem. Phys.* **1996**, *104*, 8821.
(26) Boys, S. F.; Bernardi, F. *Mol. Phys.* **1970**, *19*, 553.
(27) Carpenter, J. E.; Weinhold, F. *J. Mol. Struct.* **1988**, *169*, 41.
(28) Reed, A. E.; Curtiss, L. A.; Weinhold, F. *Chem. Rev.* **1988**, *88*, 899.
(29) Reed, A. E.; Weinstock, R. B.; Weinhold, F. *J. Chem. Phys.* **1985**, *83*, 735.
(30) Badenhoop, J. K.; Weinhold, F. *J. Chem. Phys.* **1997**, *107*, 5406.
(31) Glendening, E. D. Ph.D. Thesis, University of Wisconsin, Madison, WI, 1991.
(32) Glendening, E. D.; Weinhold, F. *J. Comput. Chem.* **1998**, *19*, 593.
(33) Glendening, E. D.; Weinhold, F. *J. Comput. Chem.* **1998**, *19*, 610.
(34) Glendening, E. D.; Badenhoop, J. K.; Weinhold, F. *J. Comput. Chem.* **1998**, *19*, 628.
(35) NBO 5.0: Glendening, E. D.; Badenhoop, J. K.; Reed, A. E.; Carpenter, J. E.; Bohmann, J. A.; Morales, C. M.; Weinhold, F., Theoretical Chemistry Institute, University of Wisconsin, Madison, WI, 2001.
(36) MOLEKEL 4.1: Flükiger, P.; Lüthi, H. P.; Portmann, S.; Weber, J., Swiss Center for Scientific Computing, Manno, Switzerland, 2000−2001.
(37) Bader, R. F. W. *Atoms in Molecules. A Quantum Theory*; Oxford University Press: Oxford, U.K., 1990.
(38) Bader, R. F. W. *Chem. Rev.* **1991**, *91*, 893.
(39) Bader, R. F. W. *J. Phys. Chem. A* **1998**, *102*, 7314.
(40) Hobza, P.; Sponer, J.; Cubero, E.; Orozco, M.; Luque, F. J. *J. Phys. Chem. B* **2000**, *104*, 6286.
(41) Popelier, P. L. A. *J. Phys. Chem. A* **1998**, *102*, 1873.
(42) Biegler-König, F.; Bader, R. F. W.; Tang, T. H. J. *J. Comput. Chem.* **1982**, *3*, 317.

Table 1. Geometric Parameters for **1**−**7**[a]

	1	2	5	3	6	4	7
R_1[b]			1.639		1.608		1.685
R_2[b]			1.724		1.733		1.684
C(2)−X(1)[c]		1.096	1.093	1.502	1.498	1.552	1.551
C(2)−O(3)		1.343	1.310	1.355	1.320	1.334	1.303
C(2)−O(4)		1.196	1.217	1.202	1.224	1.192	1.212
O(3)−H(5)		0.969	1.000	0.968	0.996	0.969	1.004
O(6)−O(7)	1.324		1.320		1.318		1.317
O(7)−H(8)	0.975		1.011		1.015		1.004
X(1)−C(2)−O(3)[c]		109.7	112.2	111.6	113.7	109.8	111.9
X(1)−C(2)−O(4)[c]		125.1	122.2	126.0	123.2	123.6	121.4
O(3)−C(2)−O(4)		125.2	125.6	122.3	123.1	126.5	126.7
C(2)−O(3)−H(5)		107.8	109.4	107.0	109.5	108.2	109.2
C(2)−O(4)−H(8)			117.9		119.6		117.2
O(4)−H(8)−O(7)			166.0		167.0		163.5
O(3)−H(5)−O(6)			168.1		169.2		168.7
H(5)−O(6)−O(7)			108.2		107.2		109.6
O(6)−O(7)−H(8)	105.5		104.8		104.4		105.0
X(1)−C(2)−O(3)−H(5)[c]		180.0	180.0	180.0	180.0	180.0	180.0
O(4)−C(2)−O(3)−H(5)		0.0	0.0	0.0	0.0	0.0	0.0
O(3)−H(5)−O(6)−O(7)			0.0		0.0		0.0
O(4)−H(8)−O(7)−O(6)			0.0		0.0		0.0
O(3)−C(2)−O(4)−H(8)			0.0		0.0		0.0

[a] Distances in angstroms, angles in degrees. [b] See Figure 1. [c] X = H for **2** and **5**; X = C for **3**−**7**.

results obtained with the former will be discussed. Figure 1 presents the numbering of atoms in the studied complexes.

Geometries. The equilibrium geometries of the complexes are planar, and their geometric parameters are similar to those obtained in former studies (Table 1).[9,12] The equilibrium geometries of the monomers in the complexes are significantly distinct from the geometries of the isolated acids and radical. The bond lengths that are most affected upon complexation are C(2)−O(3), C(2)−O(4), and O(3)−H(5) in **2**−**4** and O(7)−H(8) in **1**. The former decreases while the latter increase upon association (Table 1). The most affected bond angles are those that involve C(2) as the central atom (X(1)−C(2)−O(4) and X(1)−C(2)−O(3), where X = H for **2** and X = C for **3** and **4**) and C(2)−O(3)−H(5). The two angles involving O(3) increase, and X(1)−C(2)−O(4) decreases. The radical **1** bond angle decreases slightly upon complexation.

The perturbations in the geometry of the monomers constituting the complexes indicate that the hydrogen bonds formed between atoms O(4) and H(8) and O(6) and H(5) are of considerable strength. The directional character (linearity) of the hydrogen bonds may be a feature that allows one to distinguish between them and other electrostatic interactions.[43] The O(4)−H(8)−O(7) and O(3)−H(5)−O(6) angles in the three studied complexes present average values of 165.5° and 168.7°, respectively, indicating a trend toward linearity in these bonds. In the O(4)···H(8) hydrogen bond, the acid acts as an acceptor for the hydrogen bond, while in O(6)···H(5), the acid is the donor of the hydrogen bond (Figure 1). In **5** and **6**, R_1 is visibly shorter than R_2. R_1 and R_2 are equivalent in **7**. The latter presents the shortest distance R_2 and the longest distance R_1. The opposite occurs in **6**. In all cases, R_1 and R_2 are shorter than the distances encountered in the water dimer (∼1.95 Å) and in the formic acid−water complex (1.786 Å),[12] highlighting the great strength of such hydrogen bonds (Table 1).

Vibrational Frequencies. The comparison between the equilibrium geometries of the isolated compounds and of the monomers in the complex shows that the molecule−radical interactions are strong. A direct consequence of the structural disturbances is the alteration in the vibrational frequencies, mostly in the atoms involved in the hydrogen bonds. The stretching frequencies of the O−H, O−O, and C═O bonds in the acids and of the O−H bond in the hydroperoxyl radical were analyzed, and the data are presented in Table 2. The stretching vibrational frequencies of the C═O and O−H bonds in the isolated formic acid are in good agreement with experimental and theoretical values, showing the reliability of these results.[12,44,45]

Table 2. Vibrational Frequencies (cm^{-1}) for C═O, O−H, and O−O Stretchings[a]

	C═O	O–H (acid)	O–H (hydroperoxyl)	O–O
1			3603 (23.8)	1172
2	1818	3732 (59.8)		
5	1737	3180 (1430.4)	2949 (347.2)	1228
3	1819	3754 (60.6)		
6	1737	3214 (1520.5)	2887 (694.6)	1228
4	1862	3747 (94.9)		
7	1781	3158 (1971.4)	2995 (133.5)	1228

[a] Intensities (km/mol) are indicated in parentheses.

There is a feature of hydrogen bonds that is related to the vibrational spectrum. The frequency associated with the O−H stretching is typically red-shifted.[43,46] In the studied complexes, this shift occurs due to an increase in the O(3)−H(5) and O(7)−H(8) bond lengths, when compared to the isolated monomers, and lies between 14% and 20%. The shift in the vibrational frequency of the O(7)−H(8) stretching in **6** is relatively more pronounced than in **5** and **7**. This denotes a strong interaction and had been observed in the studies carried out by Aloísio and Francisco.[12] On the other hand, the shift in the vibrational frequency of the O(3)−H(5) stretching in **7** is higher.

The intensities of the O−H bands in acids **2**−**4** and in radical **1** also reflect the strengths of the hydrogen bonds in the studied complexes (Table 2). In complexes **5**−**7**, the intensities of the O(3)−H(5) and O(7)−H(8) stretching bands increased in relation to those encountered in the isolated monomers, as had been observed by Aloísio and Francisco.[12] The increase in the intensity of a band is due to the charge flux term,[47] which is strongly influenced by complexation. In the isolated molecule, the hydrogen charges are always positive, while the charge flux is slightly negative. Upon complexation, this term becomes positive, and therefore, both the charge and charge flux have the same algebraic signs. As the intensity of the stretching of a chemical bond is proportional to the sum of squares of these terms, the intensity of the O−H stretching increases significantly upon hydrogen bond formation.[47]

Energetic Analysis. The results obtained through the method of Xantheas[24,25] for energy decomposition are presented in Table 3. BSSE presented very low values, indicating that 6-311++G-(3df,3pd) and EPR-III basis functions adequately describe the hydrogen bond in **5**−**7**. The greatest contributions to total relaxation energies ($E_{R,total}$) are due to distortions suffered by the acids upon complex formation ($E_{R,acid}$). **4** is the acid that presents the highest E_R. Radical **1** presents the highest E_R during formation of complex **6**. This complex presents the highest total

(43) Gu, Y.; Kar, T.; Scheiner, S. *J. Am. Chem. Soc.* **1999**, *121*, 9411.
(44) Pettersson, M.; Lundell, J.; Khriachtchev, L.; Räsänen, M. *J. Am. Chem. Soc.* **1997**, *119*, 11715.
(45) Aloisio, S.; Hintze, P. E.; Vaida, V. *J. Phys. Chem. A* **2002**, *106*, 363.
(46) Scheiner, S.; Kar, T. *J. Phys. Chem. A* **2002**, *106*, 1784.
(47) Lopes, K. C.; Pereira, F. S.; de Araújo, R. C. M. U.; Ramos, M. N. *J. Mol. Struct.* **2001**, *565*−*566*, 417.

Table 3. Total ($E_{R,total}$) and Monomer ($E_{R,acid}$, $E_{R,radical}$) Relaxation Energies, Interaction Energies (Δ^2E), and Binding Energies (BE_2) (kcal/mol)

	$E_{R,acid}$[a]	$E_{R,radical}$[a]	$E_{R,total}$[a]	Δ^2E[a]	BE_2[a]	BSSE
5	1.3	0.7	2.0	−16.9	−14.9	0.4
6	1.4	0.8	2.2	−18.3	−16.1	−0.2
7	1.7	0.5	2.1	−16.6	−14.4	0.0

[a] BSSE-corrected values.

relaxation energy, indicating that its interactions are stronger than in **5** or **7**. The relaxation energies for the complexes studied herein are much higher than those calculated by Xantheas for the water dimer (0.02 kcal/mol through the MP4/aug-cc-pVTZ method).[24]

The binding energies (BE_2) and the terms of the two-body interaction (Δ^2E) once more show the stability of the complexes (Table 3), since Δ^2E values are, approximately, 4 times higher than that presented by Xantheas for the water dimer (−4.69 kcal/mol).[24] The BE_2 values for complexes **5** and **7** are practically the same, differing by 0.45 kcal/mol. The above-mentioned parameters indicate that **6** is the most stable complex among the ones studied. This is due to the electron-donor character of the methyl group. Electron donation by this group (through the inductive effect) causes an increase in the electron density, which is better accommodated by the carbonyl oxygen than by the acid O−H oxygen atom. This favors the formation of the O(4)···H(8) hydrogen bond. The higher stability of the bond formed between acetic acid and the hydroperoxyl radical has been reported in studies carried out by Francisco and Aloisio.[9,12] In complex **7**, the trifluoromethyl group (electron-withdrawing) must destabilize the O(4)···H(8) bond and stabilize the O(6)···H(5) one. The distances R_1 and R_2 help confirm this fact since this complex presents the shortest distance R_2 and the longest distance R_1, exactly the opposite of what is observed for **6**.

In most of the cases, hydrogen bond energies lie between −2 and −10 kcal/mol.[48] Some computational studies with dimers indicated that binding energies vary between −0.2 and −40 kcal/mol.[49] For the water dimer, Xantheas observed a BE_2 of −4.67 kcal/mol, which is approximately 3 times smaller than the values obtained for **5**−**7**. In a recent work, Aloisio et al. determined that one of the formic acid−water complex conformations has a binding energy of −7.0 kcal/mol,[45] i.e., more than 7.0 kcal/mol less stable than that calculated for **5**.

Atomic Charges. The atomic charges obtained through the NPA and GAPT methods are shown in Table 4. Considering the NPA charges, small variations in the atomic charges of the monomers were observed after complexation. In all three cases studied, the charges that underwent the greatest alterations were those of the oxygen atoms O(4) and O(6), which are hydrogen acceptors in the hydrogen bonds. In these two atoms, the charges became more negative when compared to the charges they had in the isolated monomers. The charge of C(2) became more positive, which can be attributed to the shift of electron density to O(4). In the same way, the charge of O(7) became less negative, probably due to an electron density shift to O(6). With respect to the charges of the hydrogen atoms that take part in the hydrogen bonds, H(5) and H(8), complexation made them more positive. The other atomic charges suffer only small alterations.

The alterations in the GAPT charges after complexation were much more intense than, and sometimes distinct from, those observed in NPA. The atomic charges of O(3), O(4), H(5), O(6), O(7), and H(8) were significantly modified. The charges of the oxygen atoms became more negative in the complex. The charges that underwent the greatest alterations were those of the hydrogen atoms taking part in the hydrogen bond, H(5) and H(8), which became more positive. The charge of C(2) should have become more positive, since O(3) and O(4) became more negative upon complexation. Nevertheless, the electron density on C(2) became higher in the studied complexes. The charges obtained through the GAPT or NPA method, or the variation in their values, do not bear any relation with the electron-donating or electron-withdrawing power of the substituents.

Second-Order Interactions between NBOs. For a better understanding of the main interactions that are involved in the stability of the isolated molecules and of the dimers, the second-order interactions between occupied and virtual natural bond orbitals were analyzed (Table 5). For open-shell systems, the unrestricted methods present distinct density matrixes, one for each spin. In this way, the interactions between NBOs are considered separately and may present pronounced differences, as observed for the methoxy and ethenoxy radicals.[50] However, the second-order interactions were similar for the radicals studied in this work.

In acids **2**−**4**, the occupied orbitals that donate electron density are the isolated pairs $\pi_{2nO(3)}$ and $\pi_{1nO(4)}$ (Figure 2), which are pure p orbitals. After hydrogen bond formation, a small s orbital (2.5−6%) contribution can be noticed in the $\pi_{1nO(4)}$ orbital. The main interactions between occupied and virtual NBOs are determined by higher $\Delta E^{(2)}$ values and correspond to $\pi_{2nO(3)} \rightarrow \pi^*_{C(2)-O(4)}$, $\pi_{1nO(4)} \rightarrow \sigma^*_{C(2)-O(3)}$, and $\pi_{1nO(4)} \rightarrow \sigma^*_{C(2)-X(1)}$ (X(1) = H(1) for **2**, and X(1) = C(1) for **3** and **4**), in order of importance. After complexation, the former is stabilized by approximately 15 kcal/mol, and the second one is destabilized by approximately 12 kcal/mol for **5** and **7** and by 16 kcal/mol for **6**. The importance of the $\pi_{2nO(3)} \rightarrow \pi^*_{C(2)-O(4)}$ interaction indicates that the carboxyl group resonance increases upon complexation. The alterations in the energy of the $\pi_{1nO(4)} \rightarrow \sigma^*_{C(2)-X(1)}$ interaction are very small. These results show that complexation with **1** leads to very similar alterations in the electronic structures of acids **5** and **7**.

The two main interactions involved in the formation of hydrogen bonds of complexes **5**−**7** are due to electron donation from the oxygen sp^2 isolated pair in acids **2**−**4** to the hydroxyl antibonding orbital in **1** ($\pi_{1nO(4)} \rightarrow \sigma^*_{O(7)-H(8)}$), and between the terminal oxygen electrons in **1** and the antibonding orbital of the O−H bond of acids **2**−**4** ($\pi_{1nO(6)} \rightarrow \sigma^*_{O(3)-H(5)}$). Similarly to what occurs in the $\pi_{1nO(4)}$ orbital, an s orbital (∼14%) contribution can be noticed in the $\pi_{1nO(6)}$ orbital of **1** after hydrogen bond formation. The stabilization provoked by the former interaction ($\pi_{1nO(4)} \rightarrow \sigma^*_{O(7)-H(8)}$) varies in the following way: **6** > **5** > **7**. For the second interaction ($\pi_{1nO(6)} \rightarrow \sigma^*_{O(3)-H(5)}$), the variation is **7** > **5** > **6**. Such observations confirm the fact that the O(7)−H(8)···O(4) hydrogen bond

(48) Pauling, L. *The Nature of the Chemical Bond and the Structure of Molecules and Crystals: An Introduction to Modern Structural Chemistry*, 3rd ed.; Cornell University Press: Ithaca, NY, 1960.
(49) Steiner, T. *Angew. Chem., Int. Ed.* **2002**, *41*, 48.
(50) Galembeck, S. E.; Nascimento, P. G. B.; Custódio, R. Submitted for publication.

Table 4. NPA and GAPT Charges

		X(1)[a]	C(2)	O(3)	O(4)	H(5)	Y(9)[b]	Y(10)[b]	Y(11)[b]	O(6)	O(7)	H(8)
1	NPA									−0.14	−0.31	0.45
	GAPT									−0.02	−0.23	0.26
2	NPA	0.11	0.66	−0.67	−0.57	0.48						
	GAPT	0.01	1.08	−0.67	−0.71	0.28						
5	NPA	0.13	0.68	−0.66	−0.63	0.49				−0.21	−0.28	0.48
	GAPT	0.03	1.04	−0.76	−0.81	0.50				−0.18	−0.33	0.53
3	NPA	−0.68	0.79	−0.69	−0.59	0.48	0.23	0.23	0.23			
	GAPT	−0.06	1.15	−0.70	−0.75	0.28	0.03	0.03	0.03			
6	NPA	−0.68	0.83	−0.68	−0.65	0.49	0.23	0.23	0.23	−0.21	−0.28	0.48
	GAPT	−0.08	1.13	−0.80	−0.87	0.50	0.03	0.04	0.04	−0.19	−0.38	0.57
4	NPA	0.97	0.70	−0.65	−0.53	0.49	−0.32	−0.33	−0.33			
	GAPT	1.56	1.02	−0.66	−0.67	0.30	−0.50	−0.52	−0.52			
7	NPA	0.97	0.73	−0.64	−0.60	0.50	−0.32	−0.33	−0.33	−0.20	−0.27	0.48
	GAPT	1.58	0.98	−0.78	−0.78	0.55	−0.50	−0.52	−0.52	−0.18	−0.33	0.52

[a] X = H for **2** and **5**; X = C for **3**−**7**. [b] Y = H for **3** and **6**; Y = F for **4** and **7**.

Table 5. Second-Order Stabilization Energies ($\Delta E^{(2)}$)

	$\Delta E^{(2)}$ (kcal/mol)										
	1			**5**			**6**			**7**	
	α	β	**2**	α	β	**3**	α	β	**4**	α	β
$\pi_{2nO(3)} \rightarrow \pi^*_{C(2)-O(4)}$			46.5	30.5	30.5	44.3	29.5	29.5	48.8	31.9	32.0
$\pi_{1nO(4)} \rightarrow \sigma^*_{C(2)-X(1)}$[a]			22.5	9.7	9.7	20.3	9.5	9.5	29.6	13.5	13.6
$\pi_{1nO(4)} \rightarrow \sigma^*_{C(2)-O(3)}$			33.1	10.6	10.6	35.3	9.6	9.7	33.7	10.9	10.9
$\sigma_{nO(4)} \rightarrow \sigma^*_{O(7)-H(8)}$				4.1	4.1		4.0	4.0		3.5	3.5
$\pi_{1nO(4)} \rightarrow \sigma^*_{O(7)-H(8)}$				12.8	12.5		15.1	14.7		9.9	9.7
$\pi_{1nO(6)} \rightarrow \sigma^*_{O(3)-H(5)}$				12.1	13.4		11.7	12.9		14.1	15.6
$\sigma_{nO(6)} \rightarrow \sigma^*_{O(7)-H(8)}$				0.7	0.7		0.7	0.7		0.7	0.8
$\pi_{1nO(6)} \rightarrow \sigma^*_{O(7)-H(8)}$	2.4	2.6		0.7	0.7		0.6	0.7		0.7	0.7

[a] X = H for **2** and **5**; X = C for **3**−**7**.

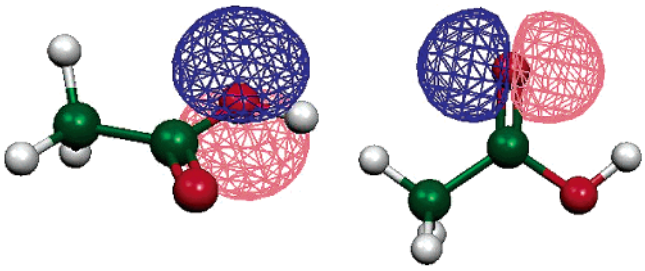

(a) *(b)*

Figure 2. NBOs: (a) $\pi_{2nO(3)}$; (b) $\pi_{1nO(4)}$.

is stronger in the complex with acetic acid (**6**) while O(3)−H(5)···O(6) is more favored in the complex with trifluoroacetic acid (**7**).

Natural Steric Analysis. NSA was used to study the interaction between the occupied or partially occupied orbitals that destabilize the monomers and dimers. This technique has been used in a study of hydrogen bonds in monomers and dimers of 2-aminoethanol.[51] The inter- or intramolecular interactions that most contribute to the destabilization of the studied systems involve a lone pair of oxygen and a vicinal bonding orbital or a lone pair of another atom. These bonding orbitals are formed through the linear bonding combination of natural hybrid orbitals (NHOs). It is interesting to observe that the antibonding combination of these NHOs is an electron-acceptor orbital for the second-order interactions according to the NBO analysis.

The interactions that most contribute to the destabilization of the isolated acids **2**−**4** and of the complexes **5**−**7** involve interactions between orbitals of isolated π pairs localized in the plane or outside it (π_{1n} or π_{2n}, respectively), with bonding orbitals located between C(2) and one of the atoms bound to it: $\pi_{2nO(3)} \leftrightarrow \pi_{C(2)-O(4)}$, $\pi_{1nO(4)} \leftrightarrow \sigma_{C(2)-O(3)}$, and $\pi_{1nO(4)} \leftrightarrow \sigma_{C(2)-X(1)}$ (X = H for **2** and **5**, and X = C for **3**, **4**, **6**, and **7**) (Table 6), where "↔" indicates a repulsive interaction. Such interactions present little variation among the noncomplexed acids **2**−**4**. Upon complexation, only a noticeable decrease in $\pi_{1nO(4)} \leftrightarrow \sigma_{C(2)-O(3)}$ occurs. In the cases of **4** and **7**, destabilizing interactions between the isolated pair orbitals of fluoro atoms and the vicinal bond orbital $\sigma_{C(1)-C(2)}$ or $\sigma_{C(1)-F}$ are observed. For radical **1**, NSA indicates that the predominant interactions occur between oxygen isolated pairs and between the isolated pair of O(6) situated in the plane of the molecule ($\pi_{1nO(6)}$) and the bonding orbital $\sigma_{O(7)-H(8)}$. The latter did not present any variation upon complexation.

Table 6. Steric Exchange Interaction Energies (d$E(i,j)$)[a]

	d$E(i,j)$ (kcal/mol)										
	1			**5**			**6**			**7**	
	α	β	**2**	α	α	**3**	α	α	**4**	α	α
$\pi_{2nO(3)} \leftrightarrow \pi_{C(2)-O(4)}$			14.3	7.6	7.5	14.5	7.6	7.6	15.3	8.1	8.0
$\sigma_{nO(3)} \leftrightarrow \sigma_{C(2)-O(4)}$			5.0	3.0	3.0	5.4	3.5	3.5	5.3	3.2	3.2
$\pi_{1nO(4)} \leftrightarrow \sigma_{C(2)-O(3)}$			12.5	3.8	3.9	14.5	4.4	4.4	12.8	4.5	4.5
$\pi_{1nO(4)} \leftrightarrow \sigma_{C(2)-X(1)}$[b]			13.3	6.3	6.3	13.0	6.6	6.6	12.6	7.2	7.2
$\sigma_{X(1)-C(2)} \leftrightarrow \sigma_{1O(3)-H(5)}$[b]							2.1	2.1	5.3	2.8	2.8
$\sigma_{nO(4)} \leftrightarrow \sigma_{C(2)-O(3)}$							3.0	2.9			
$\pi_{1nF(9)} \leftrightarrow \sigma_{X(1)-C(2)}$[b]									9.1	4.6	4.6
$\pi_{XnF(10)} \leftrightarrow \sigma_{X(1)-C(2)}$[b]									8.7	4.4	4.4
$\pi_{XnF(11)} \leftrightarrow \sigma_{X(1)-C(2)}$[b]									8.7	4.4	4.4
$\pi_{2nF(9)} \leftrightarrow \sigma_{X(1)-F(10)}$[b]									4.9	2.5	2.5
$\pi_{YnF(11)} \leftrightarrow \sigma_{X(1)-F(10)}$[b]									6.1	3.1	3.1
$\pi_{2nF(9)} \leftrightarrow \sigma_{X(1)-F(11)}$[b]									4.9	2.5	2.5
$\pi_{YnF(10)} \leftrightarrow \sigma_{X(1)-F(11)}$[b]									6.1	3.1	3.1
$\pi_{1nO(6)} \leftrightarrow \sigma_{O(3)-H(5)}$				7.2	7.6		7.0	7.4		8.3	8.7
$\sigma_{nO(4)} \leftrightarrow \sigma_{O(7)-H(8)}$				2.2	2.3		2.1	2.1		2.1	2.2
$\pi_{1nO(4)} \leftrightarrow \sigma_{O(7)-H(8)}$				8.0	8.0		9.4	9.5		6.5	6.6
$\pi_{1nO(6)} \leftrightarrow \sigma_{O(7)-H(8)}$	6.5	6.5		6.4	6.3		6.5	6.4		6.1	6.0
$\pi_{2nO(6)} \leftrightarrow \pi_{2nO(7)}$	14.8			15.2			15.2			15.2	
$\pi_{1nO(6)} \leftrightarrow \sigma_{nO(7)}$	5.1	5.3		4.5	4.7		4.6	4.7		4.4	4.5

[a] (i,j) represents the interaction between $i$and j. [b] X = H for **2** and **5**; X = C for **3**−**7**.

Some intermolecular interactions also contribute to the destabilization of the complexes. The main ones are $\pi_{1nO(6)} \leftrightarrow \sigma_{O(3)-H(5)}$ and $\pi_{1nO(4)} \leftrightarrow \sigma_{O(7)-H(8)}$. The latter is higher than the former in the cases of **5** and **6**. In the latter complex, the difference is significant (4.4 kcal/mol) if one considers the sum of energies for the interactions between orbitals α and β. The order of stability is inverted in the case of **7**. The destabilization caused by the $\pi_{1nO(4)} \leftrightarrow \sigma_{O(7)-H(8)}$ repulsion is higher in the case

(51) Vorobyov, I.; Yappert, M. C.; DuPré, D. B. *J. Phys. Chem. A* **2002**, *106*, 668.

Table 7. Spin Densities

	O(6)	O(7)		O(6)	O(7)
1	0.74	0.27	**6**	0.66	0.36
5	0.66	0.36	**7**	0.66	0.36

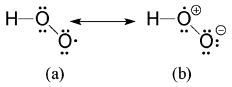

Figure 3. Main resonance structures for the hydroperoxyl radical.

of the complex with acetic acid (**6**). This can be attributed to the increase in the electron density of the carbonyl oxygen due to electron donation from the methyl group in acetic acid. An opposite effect occurs in the complex with trifluoroacetic acid (**7**), since the fluoro atoms are electron withdrawing. On the other hand, the repulsion energy due to the $\pi_{1nO(6)} \leftrightarrow \sigma_{O(3)-H(5)}$ interaction is more intense in the complex with trifluoroacetic acid. Such observations confirm the previous ones, showing that the O(7)−H(8)···O(4) hydrogen bond is stronger in **6**, while O(3)−H(5)···O(6) is stronger in **7**.

Spin Density. The spin density of the atoms of **1** has also been analyzed in this work (Table 7). The distribution of spin density in this radical, as well as its geometry and electronic structure, has been the subject of study in many theoretical and experimental works.[52] Two main resonance structures have been proposed with the aid of ab initio and semiempirical calculations.[52−57] One has the unpaired electron localized on the terminal oxygen (Figure 3a), and the other is dipolar and has the unpaired electron on the internal oxygen (Figure 3b). The latter has been previously used to explain the behavior of various peroxyl radicals.[52,58] Theoretical studies have indicated the existence of a high negative charge on the internal oxygen atom and have shown that the spin density is exclusively related to the terminal oxygen.[52,53] Experimentally, different conclusions concerning the localization of the spin density have been reached. Bower et al. concluded that there is an even spin distribution between the internal and terminal oxygen atoms.[52] Adamic et al. indicated a 2:1 ratio for spin density,[52,59] and Melamud and Silver[52,60] proposed a 0.56:0.44 ratio. The use of electron spin resonance (ESR) techniques allowed the examination of hyperfine coupling constants (HFCCs) of ^{17}O in the peroxyl radicals. In the studies carried out by Fessenden and Schuler[52,61] and Adamic et al.,[52,59] it was observed that a large majority of HFCCs are associated with the terminal oxygen. However, this could only be confirmed after the study carried out by Howard on the *tert*-butyl peroxyl radical.[52,62]

The spin densities for **1** calculated in this work are in excellent agreement with those obtained by Aplincourt et al. and Wetmore and Boyd,[11,52] and they indicate that the spin density is more related to the terminal oxygen. Complexation with acids **2**−**4** leads to a decrease in the spin density of the terminal oxygen O(6), while that of O(7) increases. Therefore, the dipolar resonance structure must be favored in **5**−**7** (Figure 3b). This observation is in agreement with the work carried out by Aplincourt et al.,[11] who verified that an increase and a decrease in the internal and external oxygen spin densities occur in aqueous solution (polar medium), respectively.

Table 8. Main Resonance Structures and Bond Orders for **2** and **5**

(**2**)		(**5**)			
	Weight (%)			Weight (%)	
		α	β	α	β
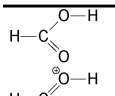	80.5	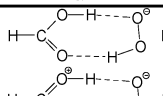	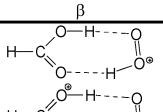	57.8	57.4
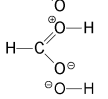	9.9	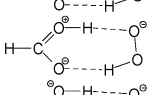	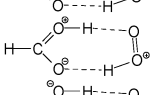	28.6	28.4
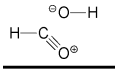	5.0	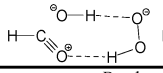	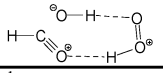	2.3	2.4

Bond orders				
	(**2**)	(**5**)		
		α	β	α + β
C(2)-H(1)	0.96	0.48	0.48	0.96
C(2)-O(3)	1.06	0.66	0.66	1.32
C(2)-O(4)	1.98	0.86	0.86	1.71
O(3)-H(5)	0.99	0.48	0.48	0.95
O(6)-O(7)	-	0.50	1.00	1.50
O(7)-H(8)	-	0.48	0.48	0.96

Table 9. Main Resonance Structures and Bond Orders for **1**

		Weight (%)	
α	β	α	β
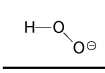	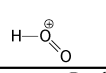	99.0	99.0

Bond orders		
	α	β
O(6)-O(7)	0.50	1.00
O(7)-H(8)	0.49	0.49
Bond orders (α + β)		
	1.51	
	0.99	

NRT Analysis. The NRT method allows the obtainment of the resonance structures that most contribute to the stability of the studied complexes. Thus, it is possible to know the alterations in the monomer canonic forms upon hydrogen bond formation. The isolated acids **2**−**4** present similar resonance structures (Table 8, Tables S8−S13 in the Supporting Information). The weight of the Lewis structures in **2** and **3** is about 80%. In the case of **4**, it is around 62%. This decrease may be attributed to the fact that in the latter compound there are a very high number of resonance structures that present little contribution, which include the trifluoromethyl group. The second resonance structure is dipolar, indicating the resonance presented by the carboxyl group.[63−65] **1** presents distinct Lewis structures for the α and β spins (Table 9). In the former case, there is a negative charge on the terminal oxygen of **1**, whereas in the latter there is a positive charge on the internal oxygen. The weight of these two Lewis structures in **1** is around 99%. The NRT analysis indicates that the resonance structure shown in Figure 3b does not contribute to **1**.

A large variation in the weight of the main canonic structures is observed upon complexation. The weight of the Lewis

(52) Wetmore, S. D.; Boyd, R. J. *J. Chem. Phys.* **1997**, *106*, 7738.
(53) Boyd, S. L.; Boyd, R. J.; Barclay, L. R. C. *J. Am. Chem. Soc.* **1990**, *112*, 5724.
(54) Liskow, D. H.; Schaefer, H. F., III; Bender, C. F. *J. Am. Chem. Soc.* **1971**, *93*, 6734.
(55) Ohkubo, K.; Fujita, T.; Sato, H. *J. Mol. Struct.* **1977**, *36*, 101.
(56) Bair, R. A.; Goddard, W. A., III. *J. Am. Chem. Soc.* **1982**, *104*, 2719.
(57) Besler, B. H.; Sevilla, M. D.; MacNeille, P. *J. Phys. Chem.* **1986**, *90*, 6446.
(58) Barclay, L. R. C.; Baskin, K. A.; Locke, S. J.; Schaefer, T. D. *Can. J. Chem.* **1987**, *65*, 2529.
(59) Adamic, K.; Ingold, K. U.; Morton, J. R. *J. Am. Chem. Soc.* **1970**, *92*, 922.
(60) Melamud, E.; Silver, B. L. *J. Phys. Chem.* **1973**, *77*, 1896.
(61) Fessenden, R. W.; Schuler, R. H. *J. Chem Phys.* **1966**, *44*, 434.
(62) Howard, J. A. *Can. J. Chem.* **1972**, *50*, 1981.
(63) Siggel, M. R. F.; Streitwieser, A., Jr.; Thomas, D. *J. Am. Chem. Soc.* **1988**, *110*, 8022.
(64) Burk, P.; Schleyer, P. v. R. *J. Mol. Struct.: THEOCHEM* **2000**, *505*, 161.
(65) Exner, O.; Cársky, P. *J. Am. Chem. Soc.* **2001**, *123*, 9564.

Table 10. Parameters from Critical Point Analysis[a]

		critical points											
		X(1)–C(2)	X(1)–Y(9)	X(1)–Y(10)	X(1)–Y(11)	C(2)–O(3)	C(2)–O(4)	O(3)–H(5)	O(6)–O(7)	O(7)–H(8)	O(4)–H(8)	O(6)–H(5)	ring HB
1	ρ_b								0.395	0.373			
	$\nabla^2\rho_b$								−0.270	−2.905			
	ϵ								0.021	0.029			
2	ρ_b	0.294				0.312	0.445	0.368					
	$\nabla^2\rho_b$	−1.118				−0.632	−0.471	−2.883					
	ϵ	0.033				0.019	0.122	0.014					
5	ρ_b	0.297				0.338	0.423	0.331	0.401	0.330	0.056	0.047	0.011
	$\nabla^2\rho_b$	−1.149				−0.657	−0.562	−2.565	−0.289	−2.560	0.102	0.093	0.051
	ϵ	0.031				0.038	0.103	0.008	0.040	0.021	0.007	0.030	
3	ρ_b	0.264	0.288	0.281	0.281	0.305	0.440	0.371					
	$\nabla^2\rho_b$	−0.684	−1.047	−0.995	−0.995	−0.667	−0.537	−2.907					
	ϵ	0.072	0.011	0.009	0.009	0.014	0.121	0.015					
6	ρ_b	0.266	0.288	0.281	0.281	0.332	0.417	0.335	0.400	0.325	0.060	0.046	0.011
	$\nabla^2\rho_b$	−0.701	−1.050	−0.997	−0.997	−0.696	−0.620	−2.607	−0.287	−2.510	0.103	0.093	0.052
	ϵ	0.073	0.011	0.011	0.011	0.031	0.099	0.010	0.040	0.021	0.009	0.032	
4	ρ_b	0.259	0.298	0.288	0.288	0.320	0.449	0.367					
	$\nabla^2\rho_b$	−0.672	−0.390	−0.407	−0.407	−0.667	−0.443	−2.915					
	ϵ	0.056	0.104	0.114	0.114	0.048	0.133	0.013					
7	ρ_b	0.261	0.298	0.290	0.290	0.346	0.428	0.325	0.402	0.337	0.049	0.051	0.011
	$\nabla^2\rho_b$	−0.683	−0.394	−0.410	−0.410	−0.687	−0.540	−2.507	−0.292	−2.648	0.104	0.092	0.050
	ϵ	0.053	0.102	0.110	0.110	0.063	0.115	0.008	0.042	0.021	0.004	0.028	

[a] X = H for **2** and **5**; X = C for **3**−**7**; Y = H for **3** and **6**; Y = F for **4** and **7**.

structures of the acids sharply decreases and that of the dipolar form increases (Table 8, Tables S8−S13 in the Supporting Information), indicating an increase in the carboxyl group resonance upon hydrogen bond formation. This suggests that the hydrogen bond has a considerable covalent character, as has been proposed in many theoretical and experimental reports.[6−8] This is so because the electrostatic interactions must have an effect only on the atoms directly involved in the hydrogen bond, and the carboxyl group resonance should not be altered. The variation in the bond orders of the carboxyl group upon complexation confirms an increment in the acid resonance. In this way, C(2)−O(3) and C(2)−O(4) are simple and double bonds in the isolated acids, but the former increases and the latter decreases in the complex. The O(6)−O(7) bond order in **1** (Table 9) does not undergo any variation upon complexation. The O−H bond orders in **1**−**4** slightly decrease after complexation.

AIM Method. The topological analysis proposed by Bader was used to obtain more information about the variation in the electron density during complexation. Additionally, the criteria proposed by Popelier for the existence of a hydrogen bond were also employed.[66] According to the latter author, the hydrogen bond must have consistent topology.[10,40,41,66−68] The electron density (ρ_b) and its Laplacian ($\nabla^2\rho_b$) of the bond critical point (BCP) must be situated in preestablished intervals. After hydrogen bond formation, one should note a charge increase ($q(\Omega)$), an energetic destabilization ($\Delta E(\Omega)$), a decrease of dipolar polarization ($M(\Omega)$), and a decrease of the hydrogen atom's volume ($v(\Omega)$). The values for the critical point (CP) analysis are presented in Table 10, while Table 11 shows the atomic properties.

1. Topology. The first condition that is necessary to confirm the presence of a hydrogen bond is the correct topology of the gradient vector field.[68] Analysis revealed the existence of BCPs between hydrogen and the acceptors of hydrogen bonds H(5)···O(6) and H(8)···O(4). Ring critical points (RCPs) are also observed for C(2)−O(3)−H(5)−O(6)−O(7)−H(8)−O(4) rings.

2. Electron Density of the Critical Point (ρ_b). This property is related to the bond order and, consequently, to the bond strength.[41,69] Complexation led to alterations in the electron densities of BCPs. An increase in ρ_b is observed for the C(2)−O(3) bond, and a decrease in this property is observed in the cases of C(2)−O(4), O(3)−H(5), and O(7)−H(8). A moderate increase in the electron density of the critical point of the O(6)−O(7) bond is also observed. These variations can be attributed to the transference of the electron density for the formation of hydrogen bonds. These data suggest that, after the occurrence of the hydrogen bond, there is an increase in the resonance of the carboxyl group, as had already been observed through the NRT analysis.

The hydrogen bonds of the complexes, O(4)···H(8) and O(6)···H(5), present values for ρ_b close to the upper limit in the interval proposed by Popelier, between 0.002 and 0.04 au[66] (Table 10). Again, it can be observed that the O(4)···H(8) bond is more favored in **6** and that O(6)···H(5) is more favored in **7**.

The ellipticity indicates the preferential charge accumulation, besides providing information about the structural stability.[41] Therefore, an increase of the ellipticity may reflect an increase in the structural instability, or even indicate an increase in the π character of the bond. The ellipticity shows that the O(4)···H(8) hydrogen bond is more stable than the O(6)···H(5) hydrogen bond (Table 10). After complexation, a decrease in the double bond character of the acid carbonyl group is observed (C(2)−O(4)), followed by an increase in the double bond character of the C(2)−O(3) and O(6)−O(7) bonds. These data reinforce the conclusion reached through the NRT analysis and through the variation in ρ_b that the hydrogen bond leads to an increase in the carboxyl group resonance. This behavior can be

(66) Popelier, P. L. A. *Atoms in Molecules: An Introduction*; Pearson Education Ltd.: Edinburgh Gate, Harlow, England, 2000.
(67) Hocquet, A. *Phys. Chem. Chem. Phys.* **2001**, *3*, 3192.
(68) Koch, U.; Popelier, P. L. A. *J. Phys. Chem.* **1995**, *99*, 9747.
(69) Wiberg, K. B.; Bader, R. F. W.; Lau, C. D. H. *J. Am. Chem. Soc.* **1987**, *109*, 1001.

Table 11. Atomic Properties[a]

		X(1)	C(2)	O(3)	O(4)	H(5)	O(6)	O(7)	H(8)	Y(9)	Y(10)	Y(11)
1	$q(\Omega)$						−0.138	−0.441	0.580			
	$M(\Omega)$						0.46	0.51	0.16			
	$v(\Omega)$						121.9	109.9	22.4			
	$-E(\Omega)$						75.189	75.407	0.377			
2	$q(\Omega)$	0.057	1.649	−1.137	−1.169	0.601						
	$M(\Omega)$	0.13	0.78	0.26	0.50	0.16						
	$v(\Omega)$	47.8	43.4	125.1	139.5	21.6						
	$-E(\Omega)$	0.606	37.003	75.908	75.973	0.355						
5	$q(\Omega)$	0.069	1.668	−1.181	−1.185	0.643	−0.215	−0.434	0.639			
	$M(\Omega)$	0.12	0.78	0.31	0.44	0.11	0.48	0.52	0.10			
	$v(\Omega)$	46.8	42.5	122.2	126.9	11.8	112.4	107.8	11.5			
	$-E(\Omega)$	0.603	36.983	75.957	75.955	0.327	75.243	75.439	0.334			
3	$q(\Omega)$	0.089	1.582	−1.139	−1.184	0.600				0.020	0.018	0.018
	$M(\Omega)$	0.11	0.81	0.24	0.46	0.16				0.13	0.13	0.13
	$v(\Omega)$	69.7	36.5	123.4	138.5	21.5				48.1	49.0	49.0
	$-E(\Omega)$	37.980	37.067	75.926	75.999	0.357				0.621	0.618	0.618
6	$q(\Omega)$	0.093	1.590	−1.188	−1.197	0.641	−0.220	−0.439	0.643	0.024	0.026	0.026
	$M(\Omega)$	0.13	0.81	0.29	0.41	0.11	0.48	0.52	0.10	0.13	0.13	0.13
	$v(\Omega)$	69.5	36.1	121.3	125.1	12.0	112.8	107.9	11.1	47.9	48.4	48.3
	$-E(\Omega)$	37.970	37.042	75.971	75.975	0.328	75.258	75.456	0.332	0.620	0.615	0.615
4	$q(\Omega)$	1.866	1.686	−1.127	−1.133	0.619				−0.640	−0.636	−0.636
	$M(\Omega)$	0.76	0.67	0.31	0.51	0.15				0.31	0.29	0.29
	$v(\Omega)$	21.3	34.3	118.9	133.5	20.6				102.5	104.1	104.1
	$-E(\Omega)$	36.744	36.995	75.889	75.944	0.345				100.378	100.359	100.359
7	$q(\Omega)$	1.879	1.708	−1.168	−1.157	0.653	−0.208	−0.424	0.637	−0.639	−0.635	−0.635
	$M(\Omega)$	0.75	0.69	0.34	0.46	0.10	0.47	0.52	0.11	0.31	0.30	0.30
	$v(\Omega)$	21.1	32.9	117.0	121.7	11.3	111.2	107.4	12.2	102.4	103.9	103.9
	$-E(\Omega)$	36.737	36.985	75.950	75.942	0.320	75.223	75.416	0.335	100.379	100.361	100.361

[a] X = H for **2** and **5**; X = C for **3**−**7**; Y = H for **3** and **6**; Y = F for **4** and **7**.

attributed to a stretching of the O(3)−H(5) bond after complexation. The distance between a BCP and an RCP can also be used as a criterion to measure the structural stability of the hydrogen bond.[41] The union of these two critical points represents a bond cleavage and the consequent ring opening.[41] The distances between the BCP of O(4)···H(8) and the RCP in **5**−**7** were 1.913, 1.914, and 1.884 Å, respectively, while the distances between the BCP of O(6)···H(5) and the RCP were 1.797, 1,761, and 1.840 Å. This is additional evidence for the fact that the O(4)···H(8) hydrogen bond is more stable than O(6)···H(5), and it allows the verification that the former is more stable in **6** and less stable in **7**, while the inverse is observed for the O(6)···H(5) bond.

3. Laplacian of the Electron Density of the Bond Critical Point ($\nabla^2\rho_b$). Both hydrogen bonds in **5**−**7** present positive values and are within the interval proposed by Popelier[41,68] (Table 10).

4. Charges ($q(\Omega)$). The charges of the hydrogen atoms involved in the hydrogen bonds, H(5) and H(8), became more positive with complexation, obeying one of the criteria proposed by Popelier[66] (Table 11). The electron density of O(3), O(4), and O(6) increased, and that of O(7) and C(2) decreased. The charges obtained through the AIM and NPA methods are qualitatively similar (Tables 4 and 11).

5. Energetic Destabilization ($\Delta E(\Omega)$). $\Delta E(\Omega)$ is defined as the difference between the energies of the atom in the complex and that in the monomer, $E(\Omega)$. Complexation stabilized the O(3), O(6), and O(7) atoms and destabilized the C(2), O(4), H(5), and H(8) atoms. The stabilization of O(6) and O(7) was higher for **3** and lower for **4**. This can be attributed to the presence of the electron-donating (CH_3) and electron-withdrawing (CF_3) groups in **3** and **4**, respectively. For the C(2) and O(4) atoms, the energetic destabilization follows the same order. Such an observation is one more evidence for the fact that the O(4)···H(8) hydrogen bond is more favored in **6**.

The formation of the hydrogen bond must promote an energetic destabilization of the donating atom of the hydrogen bond.[41] Thus, H(5) and H(8), which take part in the hydrogen bond, were destabilized. In contrast, the hydrogen atoms not involved in such bonds presented little variation in $E(\Omega)$. The same had already been observed by Popelier in the study of the dimer $(BH_3NH_3)_2$.[41]

6. Dipolar Polarization ($M(\Omega)$). The atomic integration of a position vector times the electron density gives rise to the first momentum, $M(\Omega)$.[41] The formation of the hydrogen bond leads to a loss of nonbonded density of the hydrogen atom, and consequently, a decrease in its dipolar polarization is observed.[66,68] For H(5) and H(8), there is a decrease of $M(\Omega)$ after complexation. Besides these atoms, various others presented variations of $M(\Omega)$, indicating changes in all the electronic structures of the monomers after complex formation.

7. Atomic Volume ($v(\Omega)$). The formation of the hydrogen bond must lead to a reduction in the volume of the hydrogen atom.[41,66,68] The volumes of H(5) and H(8) decreased upon complexation (Table 11), and the variations are slightly more intense in the latter. This is one more indication for the fact that O(4)···H(8) is the strongest hydrogen bond. The acceptors of hydrogen bonds, O(4) and O(6), also undergo reduction. The highest volume variation for O(4) occurs in **3** and the lowest in **4**. As for O(6), the variation of $v(\Omega)$ is the inverse of that observed for O(4). This is additional evidence for the fact that O(4)···H(8) is stronger in **6** and O(6)···H(5) is stronger in **7**.

Hydrogen Bond versus Geometric Distortion. To understand if the alterations observed in the complexes are due to distortions in the geometry of the monomers upon hydrogen bond formation, radical **1** was studied in the geometry of the

complex with formic acid (**5**). It was not possible to carry out the same comparison for **2**, since the latter was treated through restricted methods and the radicals were treated with unrestricted methods, which could lead to ambiguity in the comparison of results. As can be observed, there are remarkable differences between the properties calculated for the equilibrium structure of radical **1** and those calculated when it is complexed (Tables S14−S20 in the Supporting Information). Thus, the alterations observed in the electronic structures of the monomers when complexation occurs, such as the increment in the resonance of the carboxyl group, can be partially attributed to the hydrogen bond.

Conclusions

The complexation of the formic, acetic, and trifluoroacetic acids with the hydroperoxyl radical presents very strong hydrogen bonds. The O−H stretching band shifted to the red and was very much intensified. The energy analysis proposed by Xantheas revealed that the greater contributions to the $E_{R,total}$ values are due to distortions undergone by the acids during complex formation ($E_{R,acid}$). The NBO and NSA methods allowed the obtainment of information about the interaction between localized orbitals that most contributed to the stabilization or destabilization of the complexes. The NRT and AIM methods showed that there is an increase of the contribution of the dipolar resonance structure with complexation, as well as an increase in the resonance of the carboxyl group. A study of the properties of radical **1** in the geometry of complex **5** indicates that this increment in the resonance can be attributed to the formation of the hydrogen bond. The AIM method led to the conclusion that the formed hydrogen bonds obey the criteria established in the literature. The group of results demonstrate that the studied hydrogen bonds are strong and exert great influence on the geometric, energetic, and electronic properties of the monomers that constitute the complexes, leading to an increment in the resonance of the carboxyl group.

Acknowledgment. We thank Professor Frank Weinhold and Professor Carlos Graeff for valuable suggestions. S.E.G. thanks CNPq for a research scholarship (Grant 301957/88-6). R.L.T.P. thanks FAPESP for a Ph.D. scholarship (Grant 01/06101-6). We also thank the Laboratório de Computação Científica Avançada da Universidade de São Paulo for the generous allocation of computational resources and Ali Faiez Taha for technical support.

Supporting Information Available: Table S1, geometries calculated by UB3LYP/EPR-III, Table S2, vibrational frequencies (cm^{-1}) for C═O, O−H, and O−O stretchings, calculated by UB3LYP/EPR-III, Table S3, total ($E_{R,total}$) and monomer ($E_{R,acid}$, $E_{R,radical}$) relaxation energies, Δ^2E values, and BE_2 values (kcal/mol) calculated by UB3LYP/EPR-III, Table S4, NPA and GAPT charges calculated by UB3LYP/EPR-III, Table S5, $\Delta E^{(2)}$ values calculated by UB3LYP/EPR-III, Table S6, d$E(i,j)$ values calculated by UB3LYP/EPR-III, Table S7, spin densities calculated by UB3LYP/EPR-III, Tables S8, S9, S11, and S13, main resonance structures and bond orders for **2** and **5**, **1**, **3** and **6**, and **4**, respectively, calculated by UB3LYP/EPR-III, Tables S10 and S12, main resonance structures and bond orders for **3** and **6** and **4** and **7**, respectively, calculated by UB3LYP/6-311++G(3df,3pd), Table S14, NPA charges, Table S15, $\Delta E^{(2)}$ values, Table S16, d$E(i,j)$ values, Table S17, main resonance structures and bond orders, Table S18, spin densities, Table S19, parameters from critical point analysis, Table S20, atomic properties, Table S21, electronic energies (E) and ZPEs obtained from DFT calculations at the B3LYP (or UB3LYP for open-shell compounds)/6-311++G(3df,3pd) level, Table S22, E values and ZPEs obtained from DFT calculations at the B3LYP (or UB3LYP for open-shell compounds)/EPR-III level, Tables S23−S29, Cartesian coordinates of the optimized structures for **1**−**7** calculated by UB3LYP/6-311++G(3df,3pd), and Tables S30−S36, Cartesian coordinates of the optimized structures for **1**−**7** calculated by UB3LYP/EPR-III. This material is available free of charge via the Internet at http://pubs.acs.org.

JA036846V